Taylor & Francis
Taylor & Francis Group

Engineering Optimization

ISSN: 0305-215X (Print) 1029-0273 (Online) Journal homepage: http://www.tandfonline.com/loi/geno20

A new method to generate the ground structure in truss topology optimization

Ge Gao, Zhen-yu Liu, Yao-bin Li & Yan-feng Qiao

To cite this article: Ge Gao, Zhen-yu Liu, Yao-bin Li & Yan-feng Qiao (2016): A new method to generate the ground structure in truss topology optimization, Engineering Optimization, DOI: 10.1080/0305215X.2016.1169050

To link to this article: http://dx.doi.org/10.1080/0305215X.2016.1169050

Published online: 12 Apr 2016.

Submit your article to this journal

View related articles

View Crossmark data

Full Terms & Conditions of access and use can be found at
http://www.tandfonline.com/action/journalInformation?journalCode=geno20

Download by: [Changchun Institute of Optics, Fine Mechanics and Physics], [Ge Gao] **Date:** 13 April 2016, At: 03:22

ENGINEERING OPTIMIZATION, 2016
http://dx.doi.org/10.1080/0305215X.2016.1169050

Taylor & Francis
Taylor & Francis Group

A new method to generate the ground structure in truss topology optimization

Ge Gao[a,b], Zhen-yu Liu[a], Yao-bin Li[a] and Yan-feng Qiao[a]

[a]Changchun Institute of Optics, Fine Mechanics and Physics, Chinese Academy of Sciences, Changchun, PR China; [b]University of Chinese Academy of Sciences, Beijing, PR China

ABSTRACT

The aim of this article is to provide an effective method to generate the ground structure in truss topology optimization. The core of this method is to place nodal points for the ground structure at the intersection of the first and third principal stress trajectories, which are obtained by solving the equivalent static problem in the design domain with a homogeneous isotropic material property. It is applicable to generate the ground structure for arbitrary regular and irregular geometric design domains. The proposed method is tested on some benchmark examples in truss topology optimization. The optimization model is a standard linear programming problem based on plastic design and solved by the interior point algorithm. Compared with other methods, the proposed method may use a well-defined ground structure with fewer nodes and bars, resulting in faster solution convergence, which shows it to be efficient.

ARTICLE HISTORY
Received 2 June 2015
Accepted 15 March 2016

KEYWORDS
Ground structure; truss topology optimization; principal stress trajectories; plastic design

1. Introduction

In truss topology optimization, the main goal is to find the optimal connections between bars and to obtain the minimum weight or volume, and this approach is becoming very important in meeting growing demands with limited resources. Michell (1904) stated a fundamental design principle of plastic theory that can be used to judge whether a structure is optimal or not. However, Michell's theory does not indicate how to obtain the optimal structure. Dorn, Gomory, and Greenberg (1964) presented the ground structure method (GSM), which provides a means of obtaining approximated optimal Michell structures. In the GSM, a set of nodes, including constraint nodes and loading nodes, is chosen and connected to construct a potential truss structure (*i.e.* ground structure). Usually, areas of cross-sectional members are taken as design variables, which allows the truss topology design problem to be viewed as a sizing problem. During optimization, bars that have sufficiently small areas are deleted from the ground structure, thereby changing the topology of the truss, with the remaining bars comprising the optimal structure. However, the removal of bars with small areas may violate the stress constraint, sometimes known as stress singularity (Sved and Ginos 1968). Neglecting compatibility conditions and using approximate stress constraints can help to overcome this problem (Kirsch 1989, 1990; Rozvany 2001). Although the GSM was proposed several decades ago, it is still the main approach used for truss topology optimization today.

In general, the optimal structure is deemed to be included in the ground structure. Therefore, the more bars there are, the greater the possibility that the optimal solution is within potential connections. Usually, a better solution can be obtained by adding bars via the insertion of new nodal points.

CONTACT Zhen-yu Liu liuzy@ciomp.ac.cn

© 2016 Informa UK Limited, trading as Taylor & Francis Group

Downloaded by [Changchun Institute of Optics, Fine Mechanics and Physics], [Ge Gao] at 03:22 13 April 2016

Downloaded by [Changchun Institute of Optics, Fine Mechanics and Physics], [Ge Gao] at 03:22 13 April 2016

However, in the case of a ground structure with n nodes, there are at most $n(n-1)/2$ potential connections, which means that the number of bars increases as rapidly with n^2, leading to the 'combinatorial explosion effect'. Large-scale optimization, which must be done when large numbers of potential bars are used as design variables, is the main challenge in truss topology optimization. Gilbert and Tyas (2003) used the adaptive ground structure approach with selective subsets of active bars to solve large-scale problems that involved more than one billion bars, while Sokół (2011b, 2014) modified the approach and extended it to multiple load conditions. The reason why so many potential truss connections are needed is that nodal positions are not optimal; this is referred to as a truss geometry problem. However, adding extra nodal points can lead to many short bars and joints in the final topology and result in additional cost for the computation. Parkes (1975) proposed that a joint-length penalty be applied to each bar member to decrease the cost of fabricating the joints. Pritchard, Gilbert, and Tyas (2005) extended this method to the case of large-scale three-dimensional truss topology optimization. Dobbs and Felton (1969) proposed the technique of alternating the optimization of topology and geometry. Achtziger (2006, 2007) used an implicit mathematical programming approach to optimize truss geometry and topology simultaneously without the melting node effect. Wei, Ma, and Wang (2014) proposed a stiffness spreading method to move bar elements independently in truss layout optimization to form an optimized design. Zhou (2011) used the densities and orientations of members as variables to stimulate a truss-like continuum. Despite the efforts of many researchers to decrease bars and modify nodal positions during optimization, there seems to have been little recognition of the fact that one of the key reasons for the occurrence of the aforementioned problems is the unreasonable, predefined nodal positions in the initial ground structure. It is likely that a good result can be obtained by constructing a good ground structure with reasonable nodal point positions. However, no criteria have been proposed to judge the performance of the ground structure.

The traditional design domains for truss topology optimization are often regularly rectangular or square (Sokół 2011a). It is easy to form a mesh of mutually orthogonal families of members for these ground structures for which the optimal solution will be in accord with Michell's theory. However, practical engineering problems are often composed of arbitrary geometries rather than 'boxes', making it difficult to form mutually orthogonal members in the ground structure. Based on the finite element mesh method combined with computer-aided design software, Smith (1996, 1998) proposed an interactive system to generate ground structures in non-convex design areas. Zegard and Paulino (2014) used the ground structure analysis and design (GRAND) method to generate ground structures for unstructured design domains. However, these methods focus mainly on meshing of irregular domains rather than determining how to arrange the nodal positions reasonably, and the mesh without considering external load vectors and displacement boundary conditions may lead to undesirable optimization solutions.

Since the ground structure has a great influence on the final topology structure, the method used to generate the ground structure is very important in truss topology optimization. If a method can generate a well-defined ground structure with only a few nodes and bars, it may help to obtain a good topology solution and decrease computational cost, which is especially significant for problems in practical engineering. In this article, a new method is proposed to generate the ground structure according to the principal stress trajectories, and it is applicable to regular and irregular design domains. In addition, the nodes and bars generated by the proposed method are in locations that are more likely to be useful for truss topology optimization, and consequently this method may produce better performing structures and enhance the computational efficiency of the solution.

1.1. Background

The utilization of trajectories of the principal stresses is widespread in the design of strut-and-tie models of reinforced concrete structures (Nori and Tharval 2007; Tuchscherer, Birrcher, and Bayrak 2011), and is also suggested in many building codes (ACI 2005; BSI 1992). For example, in the reinforced concrete beams in Figure 1(a), the main steel members are configured along the principal

Downloaded by [Changchun Institute of Optics, Fine Mechanics and Physics], [Ge Gao] at 03:22 13 April 2016

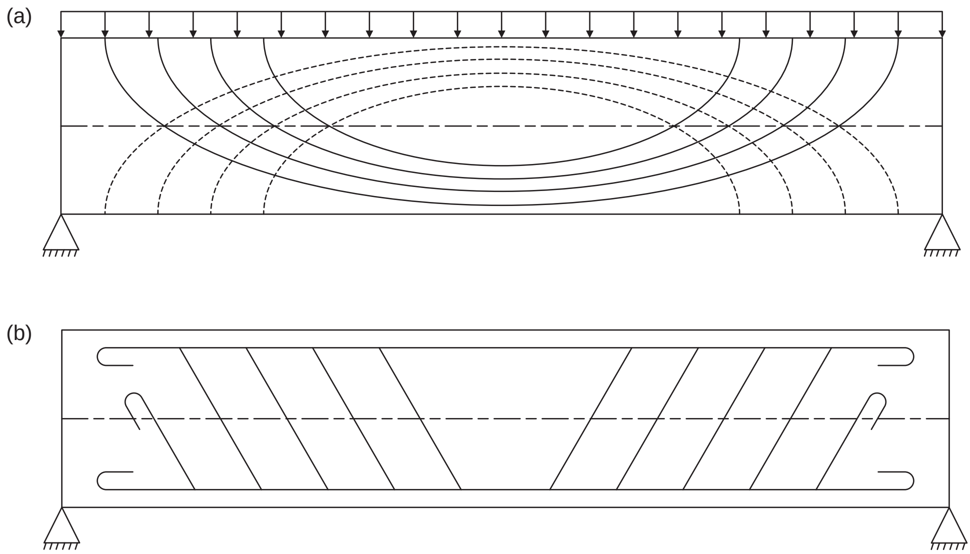

Figure 1. Reinforced concrete beams: (a) principal stress trajectories; (b) layout of steels.

trajectories of tensile stresses in order to bear stresses. As a consequence, the bearing capacity of the beams is enhanced, as shown in Figure 1(b).

In addition, it is well known that the optimal topology for a truss can be considered to be approximately the optimal force transmission path. Since the layout based on trajectories of the principal stresses proves to have a good effect on improving the capacity of structures, a new method inspired by the above ideas is proposed to generate the ground structure in truss topology optimization. In this method, the nodal points for the ground structure are placed at the intersection of the first and third principal stress trajectories. These trajectories are drawn on the basis of the stresses and strains obtained by solving the equivalent static problem in the whole design domain with a homogeneous isotropic material property.

For a plane stress problem, the first principal stress represents the maximum normal stress, while the third principal stress represents the minimum normal stress, and they are mutually orthogonal. If the trajectories are dense enough, the bars connected by nodal points at the intersection of these trajectories will be approximately orthogonal in the ground structure, meaning that the optimization solution satisfactorily meets the orthogonality condition. The approach works well for arbitrary design domains independent of geometries. At the same time, for a single loading condition, minimum compliance (or maximum stiffness) optimization is equivalent to the stress-constrained minimum volume problem (Achtziger *et al.* 1992), meaning that the stiffness increases and the volume decreases simultaneously for the structure during the optimization process. It is known that stiffness is one kind of bearing capacity. Thus, if this approach can enhance the bearing capacity of the structure, it may help to improve the stiffness (or reduce the volume) of the structure to some extent, which is compatible with the objective of the optimization. Based on the considerations above, nodal points could be placed at the intersection of the first and third principal stress trajectories to generate the ground structure, which may include good candidates for the optimal truss topology and result in a good optimization solution.

1.2. Drawing the principal stress trajectory

To obtain the principal stress trajectories, the equivalent static elastic problem in the whole design domain with a homogeneous isotropic material property is solved to obtain stress and strain values.

Downloaded by [Changchun Institute of Optics, Fine Mechanics and Physics], [Ge Gao] at 03:22 13 April 2016

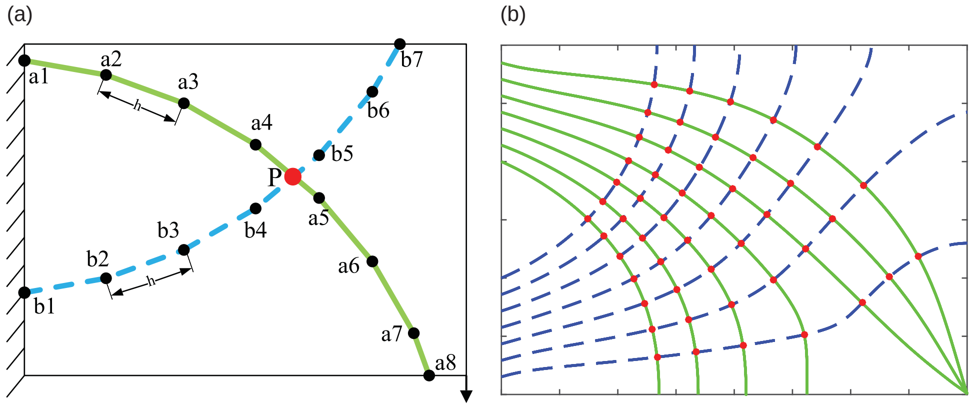

Figure 2. Simple examples: (a) two virtual principal stress trajectories; (b) several real principal stress trajectories.

This can be accomplished easily using commercial finite element method software, such as COMSOL or ANSYS. Because the accuracy of principal stress trajectories has a great influence on the optimization solution, it is suggested that higher order finite elements as well as a dense mesh be used to solve the problem in order to improve precision.

After the values and directions of the principal stresses have been obtained, the principal stress trajectories can be drawn. To illustrate a simple example in Figure 2, the steps are as follows:

(1) Select the starting points of trajectories. The points with external loads and displacement constraints are usually used. In this example, the constraint nodes a1 and b1 in Figure 2(a) are chosen as starting points.
(2) Compute the value and direction of the principal stress using Mohr's circle for the specified point.
(3) Draw a line segment with the direction above and specified constant step length h from this point to obtain the next point.
(4) Repeat steps (2) and (3).
(5) Stop when the lines reach the boundaries of the design domain. The intersection of the last line segment and the boundary is the final nodal point (*i.e.* a8 and b7).

Figure 2(b) shows several real principal stress trajectories drawn by the aforementioned steps. Note that this approach applies to the first principal stress trajectories (solid lines) as well as the third principal stress trajectories (dashed lines). The difference is that the former uses the maximum normal stress and the latter uses the minimum normal stress; subsequently, nodal points are configured at the intersection of these trajectories. Apparently, the value of step length h has a direct influence on the accuracy of the principal stress trajectories. In general, the value of h should be small enough to decrease the accumulating numerical errors. However, if it is too small, it will increase the time of drawing greatly without apparently improving accuracy. For the work described in the article, the value of h has been taken as 1/1000th of the length of the longer boundary of the design domain.

1.3. Generating the ground structure

After the intersecting nodal points have been obtained, the ground structure can be constructed by connecting these nodes. Because it is difficult to generate mesh using the discrete nodes, the methods based on mesh to construct ground structures cannot be used directly (Smith 1998; Zegard and Paulino 2014). Thus, an approach is proposed to generate the ground structure with full member connections using arbitrary distribution of the nodes.

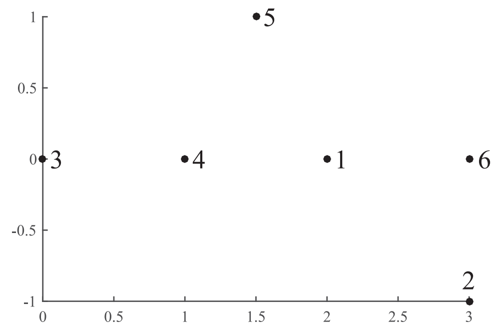

Figure 3. Six arbitrary nodal points.

The detailed procedure used to generate the ground structure is illustrated by a simple example with six arbitrary nodal points in Figure 3. Assuming that the bars with the same nodes but in a different order are regarded as different, there are $A_6^2 = 30$ member connections in total. The objective is to find the bar that connects two nodal points without others between them, which is also the basic rule for generating the ground structure. For convenience, these bars are sorted in ascending order from the starting point, and bars with the same starting point are arranged in ascending order based on the ending point, namely:

$$\text{Bar} = \begin{bmatrix} 1 & 1 & 1 & 1 & 1 & 2 & 2 & 2 & 2 & 2 & \cdots & 6 & 6 & 6 & 6 & 6 \\ 2 & 3 & 4 & 5 & 6 & 1 & 3 & 4 & 5 & 6 & & 1 & 2 & 3 & 4 & 5 \end{bmatrix} \tag{1}$$

The checking progresses among all bars with the same starting point, and the criterion for eliminating bars is the overlapping and collinear condition. For example, there are five bars starting with node 1. The steps taken to find bars connecting node 1 without overlapping and collinear members are as follows: for bar 12, by checking bars 13, 14, 15 and 16, it turns out that bar 12 has no overlapping and collinear members, so bar 12 remains in the ground structure; next, bar 13 should be checked with bars 14, 15 and 16. It is obvious that bars 13 and 14 are overlapping and collinear, so the shorter one, bar 14, remains, and the comparisons between bar 13/bar 14 and others can stop, to decrease useless computations. Bar 15 is shown to remain, by checking with bar 16. As for bar 16, it is assumed that there are no overlapping and collinear bars with this bar because it was not deleted in the previous check. As a consequence, bar 16 also remains. Thus, the bars starting with node 1 without overlapping and collinear members are bars 12, 14, 15 and 16. Figure 4 shows that the other bars are checked in the same way.

Inspired by the approach in the GRAND method (Zegard and Paulino 2014), a connectivity matrix C is proposed to find the non-repeated bars, whose row–column represents the nodal number, and

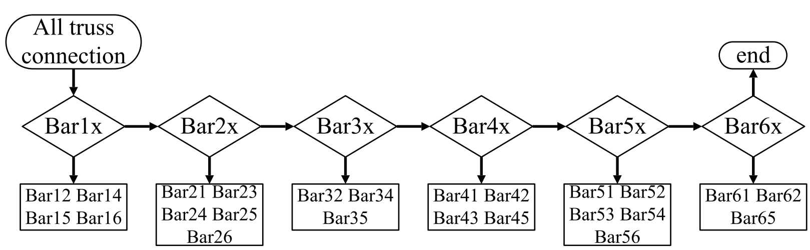

Figure 4. Overlapping and collinear bars checking progress.

Downloaded by [Changchun Institute of Optics, Fine Mechanics and Physics], [Ge Gao] at 03:22 13 April 2016

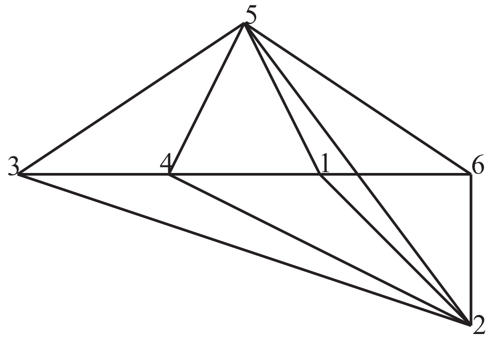

Figure 5. Connections for the ground structure.

the element value represents the existing bar member:

$$[C]_{m,n} = \begin{cases} 1 & \text{if bar with nodes } m \text{ and } n \text{ exists} \\ 0 & \text{otherwise or if } m = n \end{cases} \tag{2}$$

For this example, the connectivity matrix C obtained by the remaining bars from Figure 4 is:

$$C = \begin{bmatrix} 0 & 1 & 0 & 1 & 1 & 1 \\ 1 & 0 & 1 & 1 & 1 & 1 \\ 0 & 1 & 0 & 1 & 1 & 0 \\ 1 & 1 & 1 & 0 & 1 & 0 \\ 1 & 1 & 1 & 1 & 0 & 1 \\ 1 & 1 & 0 & 0 & 1 & 0 \end{bmatrix} \tag{3}$$

It is worth noting that if the checking progress is correct, the connectivity matrix C is symmetrical, and its upper triangular part is just the connectivity of non-repeated bars. Thus, the 12 non-overlapping bars in Equation (4) finally generate the ground structure, which is shown in Figure 5.

$$\text{Bar} = \begin{bmatrix} 1 & 1 & 1 & 1 & 2 & 2 & 2 & 2 & 3 & 3 & 4 & 5 \\ 2 & 4 & 5 & 6 & 3 & 4 & 5 & 6 & 4 & 5 & 5 & 6 \end{bmatrix} \tag{4}$$

This approach can generate the ground structure with full connections independent of nodal positions and numbers, especially for irregular design domains. It is notable that the ground structure obtained in this way is a convex polygon. That is to say, if the original design domain is convex, this method can be used to generate the ground structure directly. But if the design domain is concave, this method should be used in conjunction with the collision-detection technique (Bergen 2004; Ericson 2004) to delete unexpected members that lie in concave zones.

1.4. Collision-detection technique

The collision-detection technique is widely used in the games industry and in computational geometry (Bergen 2004; Ericson 2004). Generally speaking, it provides some algorithms to help judge the collision between two objects. For truss topology optimization, these algorithms are used to eliminate unexpected bars which lie outside the design domain when constructing the ground structure. The L-beam problem is used here as a demonstration.

The design domain of the L-beam problem is shown in Figure 6(a), where the points represent nodes in the ground structure. Figure 6(b) shows the ground structure with full connections by the method proposed above. Bars 51, 53, 54, 81, 82 and 83 are unexpected members which lie outside

Downloaded by [Changchun Institute of Optics, Fine Mechanics and Physics], [Ge Gao] at 03:22 13 April 2016

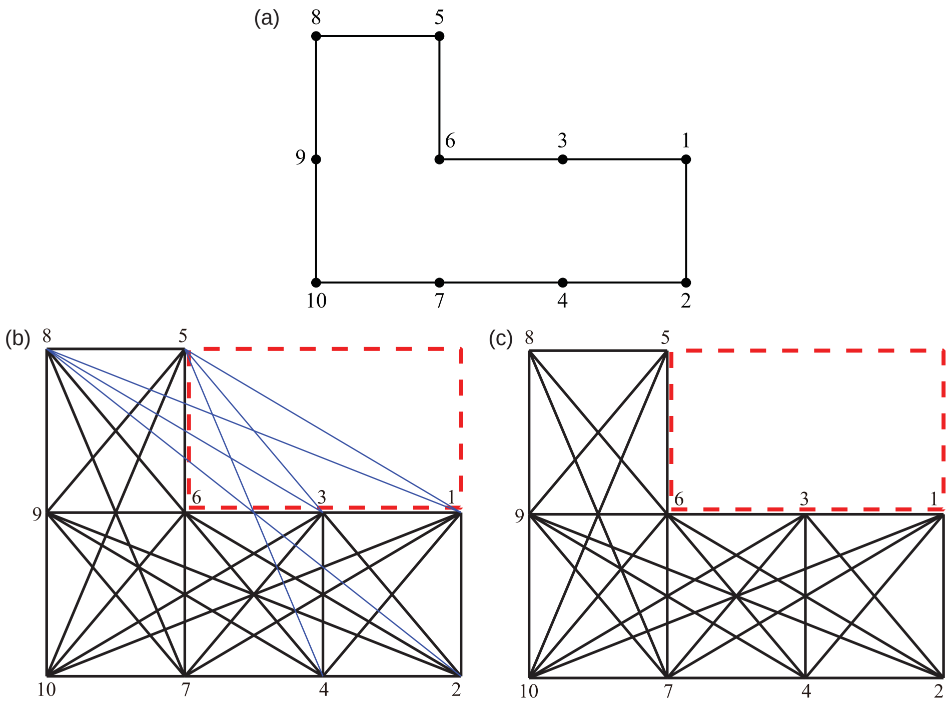

Figure 6. L-beam problem: (a) original node distribution; (b) connections without collision-detection technique; (c) connections with collision-detection technique.

the design domain. It is worth noting that these five bars intersect with the dashed rectangle, which is usually called the restriction zone (Zegard and Paulino 2014), and others lying in the design domain do not. Therefore, it merely needs to judge whether the bars in the ground structure with full connections intersect with the restriction zone (a line segment against a rectangle in this example), and then eliminate intersecting members. Figure 6(c) shows the final ground structure constructed by the remaining bars, where all members lie within the design domain. The numerical algorithms or criteria used to judge the collision with restriction zones are called the collision-detection technique. With the help of this approach, the ground structure for concave design domains can be successfully constructed.

2. Formulation

The work reported in this article focuses on plastic design in which only a stress (strength) condition is prescribed and elastic compatibility is not required (Hemp 1973; Rozvany 2011). As mentioned above, for a single loading condition, optimization of the maximum stiffness is equivalent to the stress-constrained minimum volume problem. The optimal result is known to be statically determinate, and therefore the optimal solution for these structures is equally valid for optimal elastic and plastic designs (Rozvany 1997; Rozvany, Sokół, and Pomezanski 2014). In addition, the plastic design for one load case is free from the stress singularity problem (Kirsch 1989, 1990).

The basic formulation of the stress-constrained, minimum-volume problem in plastic design, neglecting the compatibility condition, is (Bendsøe and Sigmund 2003):

$$\min_{\boldsymbol{f},\boldsymbol{v}} \quad \sum_{e=1}^{M} v_e$$

Downloaded by [Changchun Institute of Optics, Fine Mechanics and Physics], [Ge Gao] at 03:22 13 April 2016

Downloaded by [Changchun Institute of Optics, Fine Mechanics and Physics], [Ge Gao] at 03:22 13 April 2016

$$\begin{aligned} \text{s.t.:} \quad & \boldsymbol{Bf} = \boldsymbol{F} \\ & -\overline{\sigma_C} v_e \le l_e f_e \le \overline{\sigma_T} v_e, \quad e = 1, \ldots M \\ & v_e \ge 0, \qquad\qquad\qquad e = 1, \ldots M \end{aligned} \tag{5}$$

where v_e and f_e are the volume and axial force of the *eth* truss member, respectively. $\boldsymbol{M}$ is the total number of members, $\boldsymbol{F}$ is the nodal force vector with size $N \times 1$, where N denotes the number of degrees of freedom. $\boldsymbol{B}$ is the compatibility matrix with size $M \times N$, the *ith* column of which is $[0, \ldots, -C_{ax}^{(i)}, -C_{ay}^{(i)}, 0, \ldots, C_{bx}^{(i)}, C_{by}^{(i)}, 0, \ldots]^{\mathrm{T}}$. Here, C_x and C_y refer to the cosines of the x-direction and y-direction of the ith member with starting point a and ending point b, respectively. For a stable ground structure, $\boldsymbol{B}$ has full ranks N $(N \le m)$. The terms $\overline{\sigma_T}$ and $\overline{\sigma_C}$ refer to the stress limits in tension and compression, respectively.

It is worth noting that the stress constraints are written in terms of force. To obtain a fully stressed design, the expressions of volume and axial force are modified as follows (Bendsøe and Sigmund 2003):

$$\begin{aligned} v_e &= l_e \left(\frac{f_e^+}{\overline{\sigma_T}} + \frac{f_e^-}{\overline{\sigma_C}} \right) \\ \boldsymbol{f} &= \boldsymbol{f}^+ - \boldsymbol{f}^- \end{aligned} \tag{6}$$

Then, the formulation of the optimization problem is changed to a standard linear programming (LP) problem:

$$\begin{aligned} \min_{f^+, f^-} \quad & \sum_{e=1}^{M} l_e \left(\frac{f_e^+}{\overline{\sigma_T}} + \frac{f_e^-}{\overline{\sigma_C}} \right) \\ \text{s.t.:} \quad & \boldsymbol{B}(\boldsymbol{f}^+ - \boldsymbol{f}^-) = \boldsymbol{F} \\ & f_e^+ \ge 0, f_e^- \ge 0, \quad e = 1, \ldots M \end{aligned} \tag{7}$$

where the design variables are axial forces only, and f_e^+ and f_e^- can be seen as the eth member tension and compression, respectively, and at least one of them is zero. The axial force is tension if $f_e^- = 0, f_e^+ > 0$ and compression if $f_e^- > 0, f_e^+ = 0$. In the case where $f_e^- = 0, f_e^+ = 0$, it is assumed that the bar can be deleted from the connections of the ground structure. It is easy to achieve a global optimal solution for the LP problem using the interior point algorithm (Luenberger and Ye 2008). It is notable that the above LP problem can also be handled with the adaptive GSM (Gilbert and Tyas 2003; Sokół 2011b, 2014), which is much more effective for large-scale problems. However, the direct method is chosen in this article because the numerical examples used are just medium-scale problems.

3. Numerical examples

The following benchmark examples are solved to show the effectiveness of the proposed method. Unless stated otherwise, the parameters used to draw the trajectories of the principal stresses are defined as follows: Poisson's ratio $\nu = 0.33$, Young's modulus $E = 2 \times 10^{11}$ Pa and external load $P = 1$ N. The optimization of the truss topology is based on equal stress limits for tension and compression, meaning $\sigma_{\mathrm{T}} = 1$ and $\sigma_C = 1$. The equivalent static problem in the design domain is solved by commercial software COMSOL3.5 with the Lagrange–quadratic element to draw the trajectories of the principal stresses and to optimize the topology of the trusses. All problems are tested on an Intel i5 M 560 personal computer running at 2.67 GHz with 4 GB of RAM.

Downloaded by [Changchun Institute of Optics, Fine Mechanics and Physics], [Ge Gao] at 03:22 13 April 2016

3.1. Irregular design domain

A well-known example of truss optimization in the irregular design domain is the Michell cantilever, for which loading and boundary conditions are shown in Figure 7. Unlike the 'box' zones, the design domain has circular support, making it complicated to construct the ground structure with mutually orthogonal bars in traditional ways. If the height b of the domain is long enough, the analytical optimal volume is $V_{\text{opt}} = \text{Pa} \log(a/r)(1/\overline{\sigma_T} + 1/\overline{\sigma_C}) = 16.0944$ (Michell 1904).

In this example, the starting points of the principal stress trajectories are equally distributed on the circular boundary. Because too few principal stress trajectories cannot reflect the real stress distribution, which has a great influence on the optimal solution, it is suggested that the trajectories be drawn densely enough to generate the ground structure. Cases of different numbers of principal stress trajectories are listed in Figure 8, where N is the number of each kind of principal stress trajectory. The solid lines represent the first principal stress trajectories and the dashed lines represent the third principal stress trajectories. The intersections of these trajectories are used as the nodes that connect the bars in the ground structure.

Ground structures will be constructed using these nodes via the approach presented in Section 1.3. The ground structure for $N = 12$ is shown in Figure 9. It can be seen that the design domain has a concave region (*i.e.* the circular support zone). The bars that intersect with the half-circle are unexpected ones, all or part of which are outside the design domain in Figure 9(a). Therefore, in the collision-detection algorithm a line segment against a circle is used to eliminate redundant bars, and the remaining members generate the final ground structure in Figure 9(b).

The optimum topology solutions for these ground structures are listed in Figure 10, and the detailed optimization information is listed in Table 1, where T_{LP} presents the time taken by the central processing unit (CPU) to solve the LP problem. The bars for optimal structures are just along the principal stress trajectories. If these principal stress trajectories are drawn densely enough, the final optimization solution can meet the orthogonality condition. It is worth noting that the optimal value of the volume decreases as the number of principal stress trajectories increases, and the topology structure becomes more and more similar to the analytical structure (Michell 1904). In the case in which 24 trajectories are used to generate the ground structure, the minimum volume obtained is 16.2065, where the relative error is merely 0.7% compared with the analytical solution. In addition, the topology structures are very brief and clear, without unnecessary irregular members.

For the sake of comparison, the same problem is solved using the ground structure generated via the GRAND method (Zegard and Paulino 2014). Table 2 presents the solutions of various numbers of elements with the constant parameters $MaxIter = 20$ and $Lvl = 25$. Figure 11 shows the mesh and topology structure by $NElem = 500$. From the data in Tables 1 and 2, it can be found that the proposed method can use fewer nodes and bars to generate a well-defined ground structure and obtain a similar

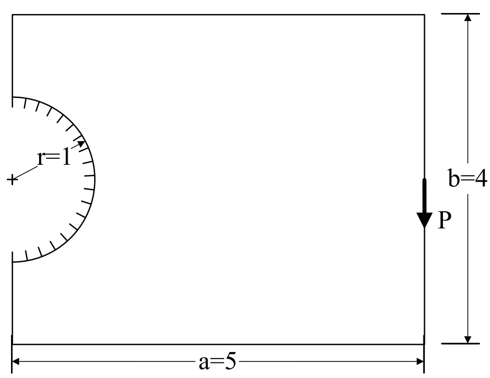

Figure 7. Michell cantilever problem.

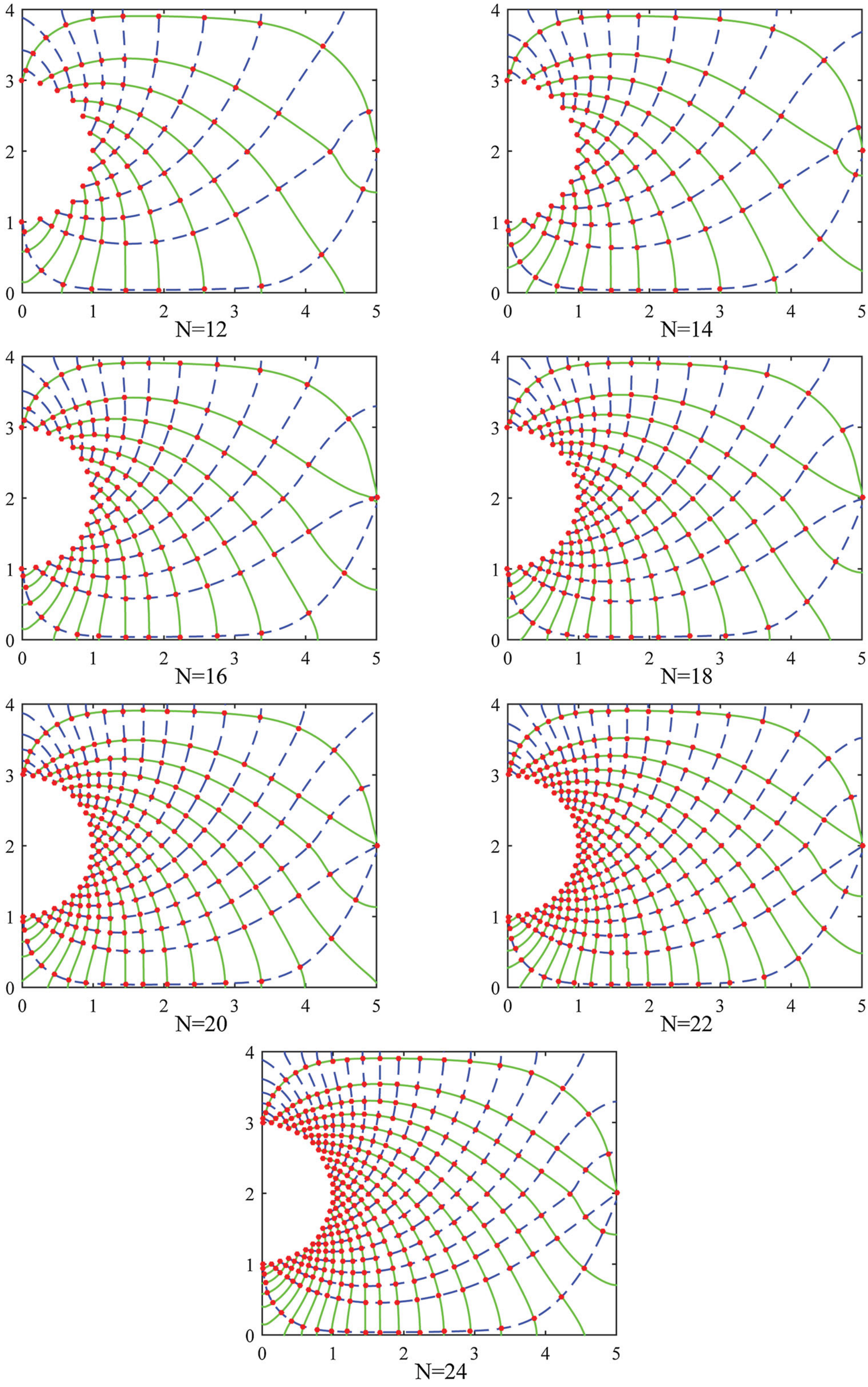

Figure 8. Different numbers of principal stress trajectories for the Michell cantilever.

Downloaded by [Changchun Institute of Optics, Fine Mechanics and Physics], [Ge Gao] at 03:22 13 April 2016

Downloaded by [Changchun Institute of Optics, Fine Mechanics and Physics], [Ge Gao] at 03:22 13 April 2016

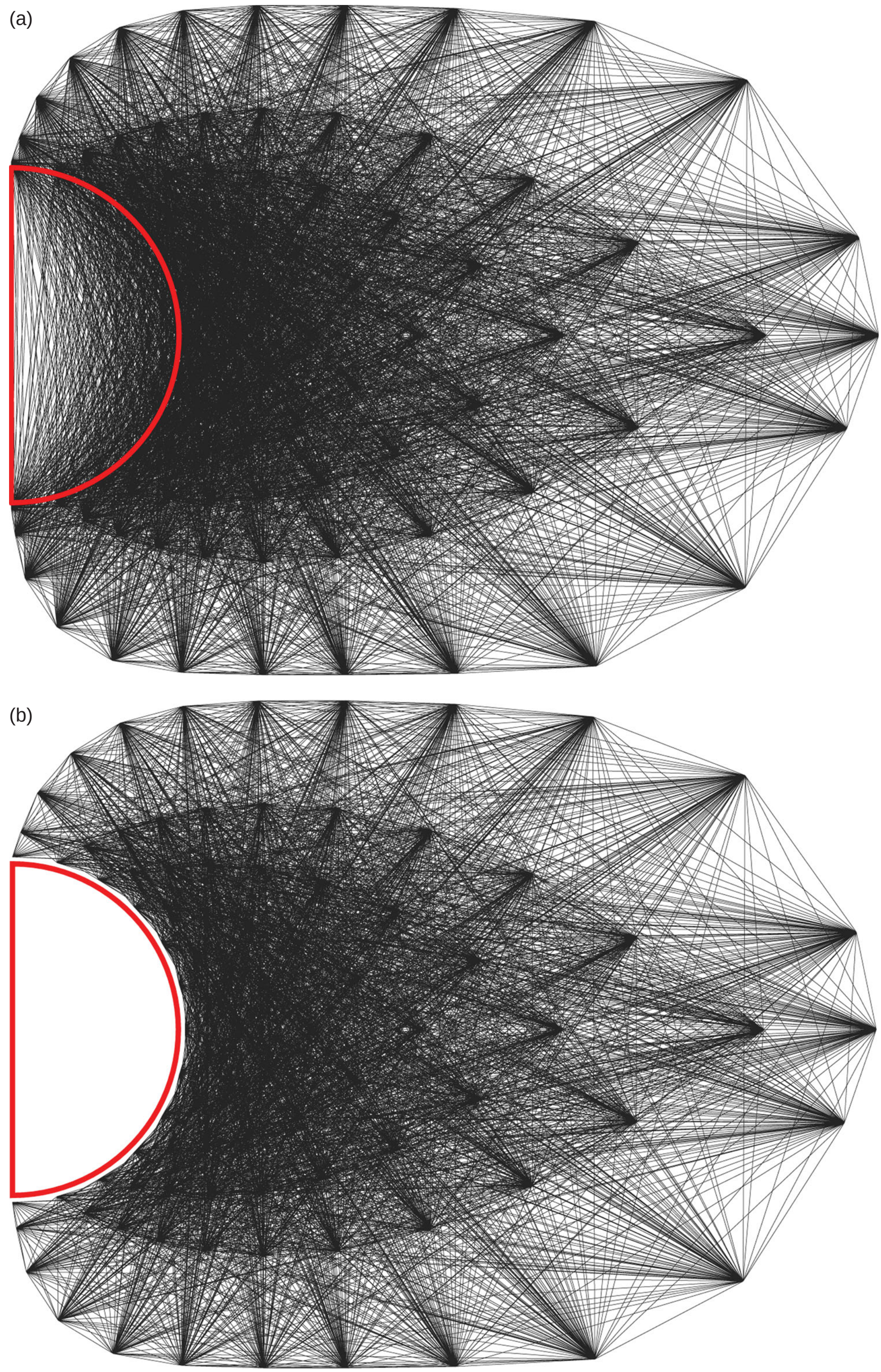

Figure 9. Ground structure for $N = 12$: (a) convex ground structure; (b) concave ground structure.

Downloaded by [Changchun Institute of Optics, Fine Mechanics and Physics], [Ge Gao] at 03:22 13 April 2016

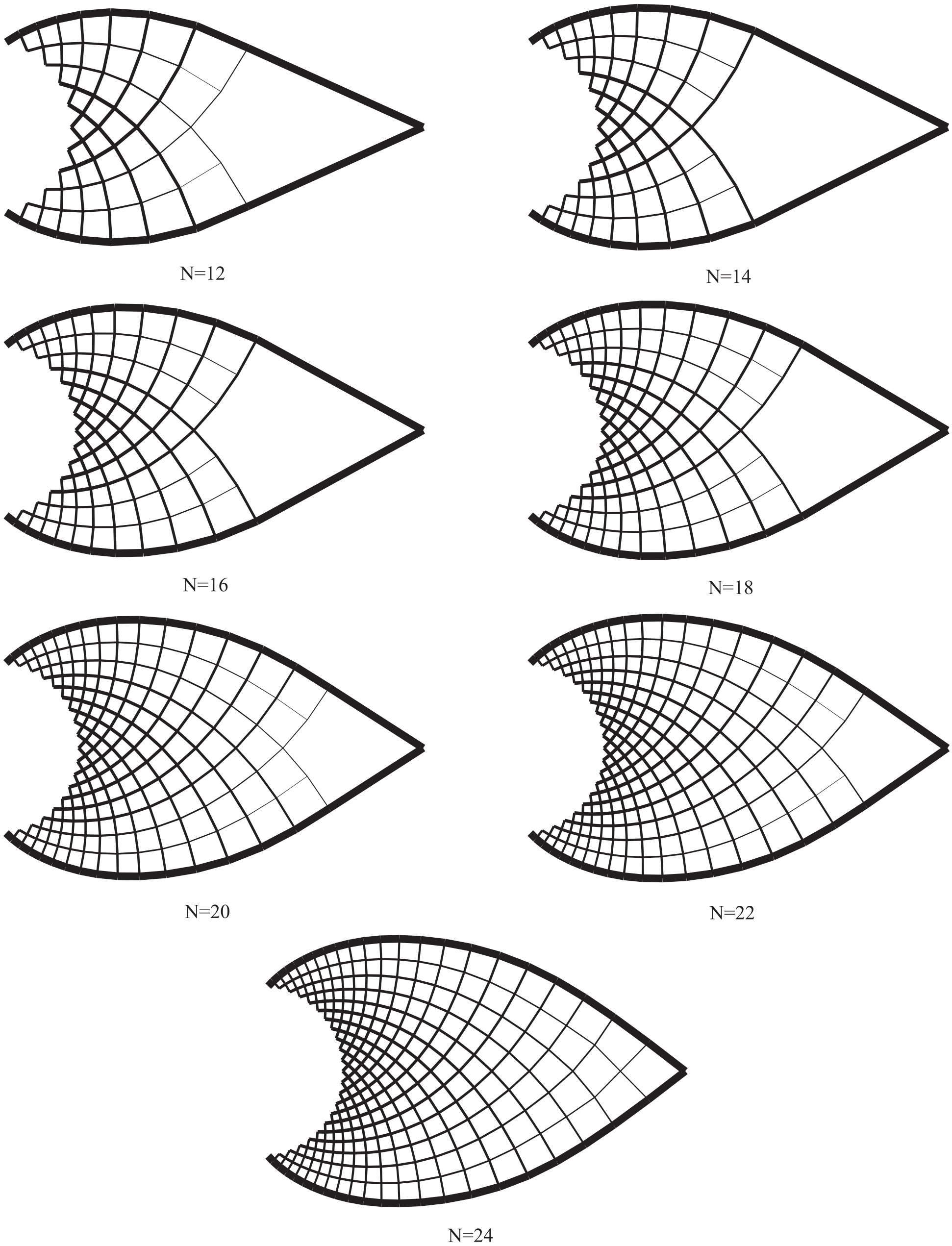

Figure 10. Optimum solutions of different numbers of trajectories for the Michell cantilever.

volume value compared with this popular mesh method, and consequently less CPU time for solving the LP problems to result in faster solution convergence. In addition, in approximately the same volume (with relative error 0.7%), the topology structure obtained by the new method in Figure 10 ($N = 24$) is simpler and clearer, without unnecessary bars with near-zero area, compared with the result in Figure 11(b). From the above observations , one may conclude that the new approach can generate well-defined ground structures for irregular design domains which include good candidates for the optimal topology structure, leading to better optimization solutions.

Table 1. Solutions of different trajectories for the Michell cantilever.

Number	Node	Bar	Volume	Error	T_{LP} (s)
12	91	3,222	16.8519	4.71%	0.290826
14	120	5,745	16.6076	3.19%	0.518796
16	151	9,135	16.4487	2.20%	0.827591
18	187	14,168	16.3485	1.58%	1.53509
20	228	21,197	16.2791	1.15%	2.69551
22	273	30,635	16.2348	0.87%	4.09549
24	322	42,842	16.2065	0.70%	6.69554

Table 2. Solutions of different elements for the Michell cantilever by ground structure analysis and design (GRAND).

NElem	Node	Bar	Volume	Error	T_{LP} (s)
40	86	3,292	16.8734	4.84%	0.364764
70	143	9,181	16.6006	3.15%	1.1523
100	200	17,943	16.4121	1.97%	3.49436
200	394	67,431	16.2736	1.11%	23.6787
300	592	145,490	16.2369	0.89%	74.5118
400	794	249,054	16.2188	0.77%	189.686
500	994	371,079	16.2075	0.70%	347.925

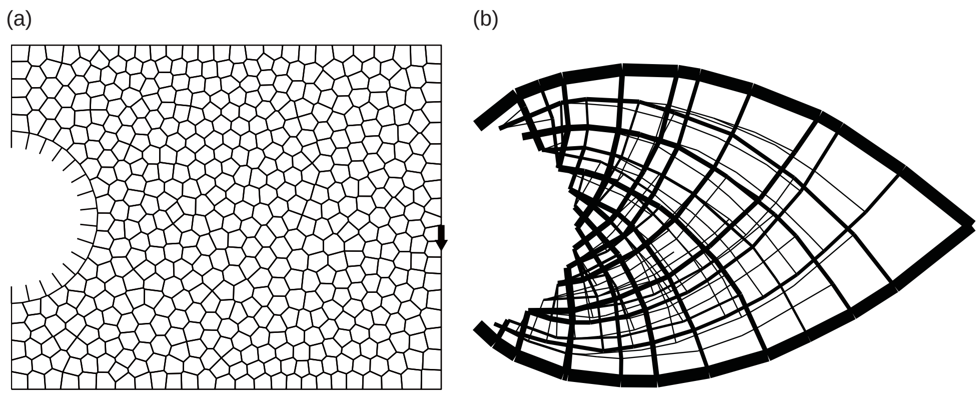

Figure 11. Michell cantilever topology optimization by ground structure analysis and design (GRAND) for *NElem* $= 500$: (a) finite element method mesh for the design domain; (b) optimum topology.

3.2. Regular design domain

This method is applicable to regular design domains as well. The Bridge problem is illustrated as an example, with the loading and boundary conditions shown in Figure 12. The analytical optimal volume is $V_{\text{opt}} = P(a/2)(1/2 + \pi/4)(1/\overline{\sigma_T} + 1/\overline{\sigma_C}) = 3.8562$ (Michell 1904).

In this example, points around loading and constraint nodes are chosen as the starting points of the trajectories of the principal stresses. The structure in this example is symmetrical for axis $x = 1.5$, which means that only half of the trajectories need to be drawn, and the rest can be obtained using a symmetry operation. Topology solutions of different numbers of principal stress trajectories are listed in Table 3, where Nf and Nt represent the number of the first and the third principal stress trajectories, respectively. Again, the volume value becomes smaller and smaller with the increasing number of trajectories. In the case of $Nt = 11$ and $Nf = 12$, the optimal volume is 3.8652 with relative error 0.23%. The distribution of principal stress trajectories and the optimum solution for this case are shown in Figure 13(a) and (b), respectively. Note that the bars in the topology structure are approximately along the principal stress trajectories.

Downloaded by [Changchun Institute of Optics, Fine Mechanics and Physics], [Ge Gao] at 03:22 13 April 2016

Downloaded by [Changchun Institute of Optics, Fine Mechanics and Physics], [Ge Gao] at 03:22 13 April 2016

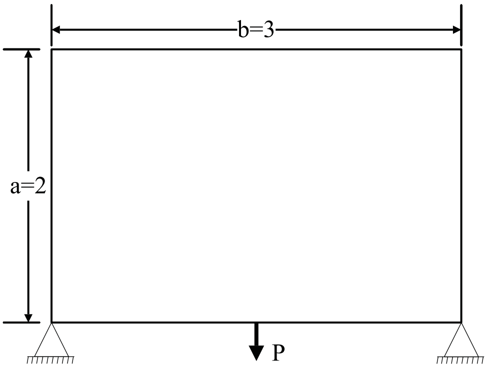

Figure 12. Bridge problem.

Table 3. Solutions of different trajectories for the Bridge problem.

Nt	*Nf*	Node	Bar	Volume	Error	T_{LP} (s)
7	4	52	1,304	3.8984	1.09%	0.13718
8	6	91	4,066	3.8743	0.47%	0.396737
9	8	138	9,416	3.8674	0.29%	1.28103
10	11	211	22,109	3.8670	0.28%	3.82562
11	12	250	31,069	3.8652	0.23%	5.40863

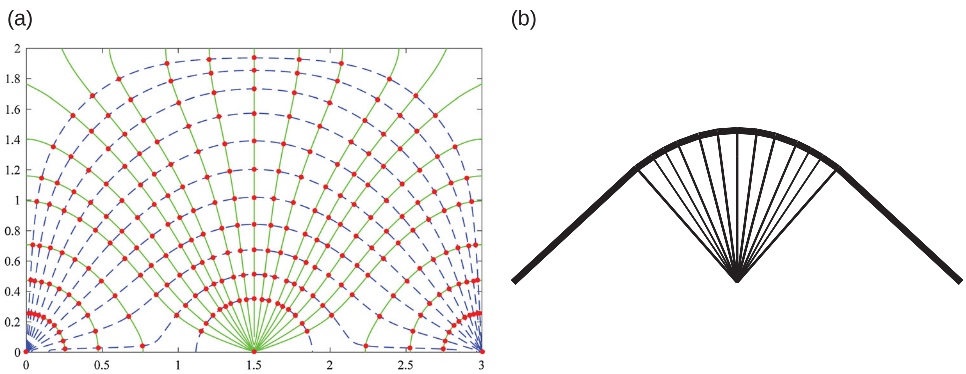

Figure 13. Case of $Nt = 11$ and $Nf = 12$ for the Bridge problem: (a) principal stress trajectories distribution; (b) optimum solution.

The problem is also optimized by the traditional method with square mesh division and full connections, which can easily form mutually orthogonal bars. Table 4 provides optimization information about different meshes for the ground structures. From the data in Tables 3 and 4, the observation can be made that in order to obtain a similar volume value, there are fewer nodes and bars in the ground structure generated by the new method. In the case of a volume value with error of about 0.24%, the ground structure of mesh 48×32 in Figure 14(a) must be used, which has more bars (795,804) than the new method (31,069), thus inevitably increasing the computational cost for solving the LP problem. In addition, Figure 14(b) shows that the optimized topology has no vertical bar that is independent of the number of meshes used. However, such a vertical member exists in the topology that is optimized by the new method in Figure 13(b), which is in agreement with the analytical solution. Therefore, the new proposed method can generate a well-defined ground structure whose nodes and bars are more likely to be useful for truss topology optimization, which can result in good performance structures for the regular design domains as well.

Table 4. Solutions of different mesh divisions for the Bridge problem.

Mesh	Node	Bar	Volume	Error	T_{LP} (s)
18×12	247	18,622	3.9048	1.26%	2.91788
24×16	425	55,024	3.8964	1.04%	15.6073
30×20	651	129,182	3.8801	0.62%	55.9815
36×24	925	260,468	3.8742	0.47%	166.688
42×28	1247	472,822	3.8693	0.34%	427.410
48×32	1617	795,804	3.8656	0.24%	1014.71

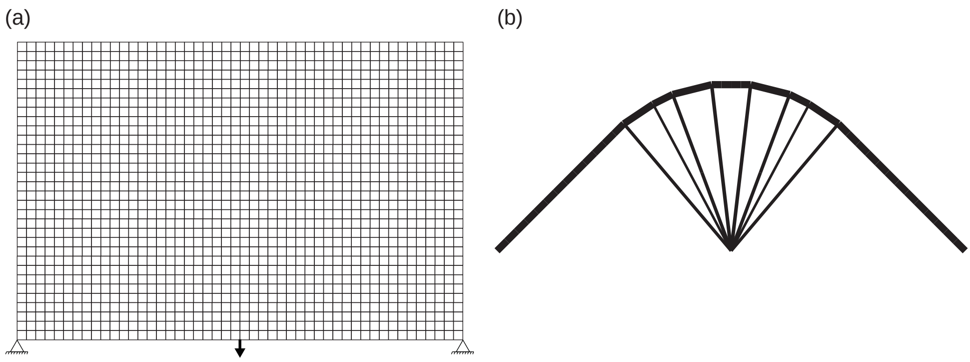

Figure 14. Bridge topology optimization by mesh 48×32: (a) design domain mesh; (b) optimum topology.

Downloaded by [Changchun Institute of Optics, Fine Mechanics and Physics], [Ge Gao] at 03:22 13 April 2016

4. Discussion

The above examples show that the proposed method can generate well-defined ground structures with only a few nodes and bars for truss topology optimization, with equal permissible stresses in tension and compression. However, in plastic design, especially for structures with statically indeterminate support conditions (Rozvany 1996; Sokół and Rozvany 2013), the stress limit ratio ($\kappa = \sigma_T/\sigma_C$) has an effect on the optimal structure; in this case, the trajectories have to be changed to obtain good solutions for different stresses in tension and compression. One possible approach is to use the dual extension/compression modulus model to establish the nonlinear relationship between stress and modulus (Liu and Qiao 2011), the elasticity parameters of which can be adjusted depending on the stress limit ratio. In this way, the layout of trajectories of principal stresses may be adjusted reasonably for different stresses in tension and compression, and lead to good topology structures. In addition, owing to the difference in properties, it is worth noting that the trajectories of principal stresses for isotropic material may not be optimal for orthotropic material defined by Michell structures. Nevertheless, combined with shape optimization (Achtziger 2006, 2007), the position of nodal points generated by the proposed method for design domains with orthotropic material can also be better adjusted to construct good ground structures. Moreover, although not considered here, the method may be extended to multi-load case problems in plastic design, whose trajectories of principal stresses can be obtained by superposition of the trajectories of principal stresses that were obtained in the one-load case on the basis of component loads (Nagtegaal and Prager 1973; Rozvany, Sokół, and Pomezanski 2014; Sokół 2014). In this case, it is suggested that the adaptive GSM is used to solve the large-scale LP problems, and this proves to be efficient and reliable (Gilbert and Tyas 2003; Sokół 2011b, 2014).

This article provides an algorithm to construct the ground structure with full connections and without overlapping members, using arbitrary nodes. However, it is obvious that it can be simplified and improved by other, more efficient methods. Furthermore, the forward integration method used to draw trajectories is not accurate enough and costs additional time, which could be improved by more accurate approaches (*e.g.* Xu and Yuan 2005) and should be realized automatically to improve the accuracy and efficiency in future research.

5. Conclusion

An efficient new method is proposed to generate the ground structure in truss topology optimization in plastic design. Unlike traditional ways, which use the relationship between nodes and mesh to construct ground structures, the proposed method uses the intersections of the trajectories of the first and third principal stresses as nodal points to generate the ground structure, which are obtained by solving the equivalent static problem in the whole design domain with a homogeneous isotropic material property. There are some merits to this method. First, this approach can be applied to arbitrarily shaped design domains. The bars constructed in the ground structure can be approximately orthogonal if there are dense enough principal stress trajectories, independent of the geometry of the zones. Secondly, the nodes and bars generated for the ground structure are more likely to be in reasonable locations that may help to construct useful bars for truss topology optimization. Thus, the proposed method may generate well-defined ground structures with only a few nodes and bars, resulting in structures with good performance, which shows that it can enhance the computational efficiency of the solution.

Disclosure statement

No potential conflict of interest was reported by the authors.

Funding

This work was supported by the Science and Technology Development Plan of Jilin Province [grant no. 20140519007JH] and National Natural Science Foundation of China [grant no. 51275504].

ORCID

Ge Gao http://orcid.org/0000-0002-0071-5837
Zhenyu Liu http://orcid.org/0000-0002-3090-185X
Yaobin Li http://orcid.org/0000-0001-7046-2655
Yanfeng Qiao http://orcid.org/0000-0002-5424-2545

References

Achtziger, W. 2006. "Simultaneous Optimization of Truss Topology and Geometry, Revisited." In *IUTAM Symposium on Topological Design Optimization of Structures, Machines and Materials: Status and Perspectives*, edited by M. P. Bendsøe, N. Olhoff, and O. Sigmund, 413–423. Dordrecht: Springer.

Achtziger, W. 2007. "On Simultaneous Optimization of Truss Geometry and Topology." *Structural and Multidisciplinary Optimization* 33 (4–5): 285–304.

Achtziger, W., M. Bendsøe, A. Ben-Tal, and J. Zowe. 1992. "Equivalent Displacement Based Formulations for Maximum Strength Truss Topology Design." *Impact of Computing in Science and Engineering* 4 (92): 315–345.

American Concrete Institute (ACI). 2005. *ACI Committee 318. Building Code Requirements for Reinforced Concrete and Commentary (ACI 318M-05)*. United States.

Bendsøe, M. P., and O. Sigmund. 2003. *Topology Optimization: Theory, Methods and Applications*. Berlin: Springer.

Bergen, G. 2004. *Collision Detection in Interactive 3D Environments*. San Francisco: Morgan Kaufmann.

British Standards Institution (BSI). 1992. *Eurocode 2: Design of Concrete Structures—Part 1-1: General Rules and Rules for Buildings*. United Kingdom.

Dobbs, M. W., and L. P. Felton. 1969. "Optimization of Truss Geometry." *Asce Journal of Structural Division* 95: 2105–2118.

Dorn, W., R. Gomory, and H. Greenberg. 1964. "Automatic Design of Optimal Structures." *Journal de Mecanique* 3 (1): 25–52.

Ericson, C. 2004. *Real-Time Collision Detection*. San Francisco: Morgan Kaufmann.

Downloaded by [Changchun Institute of Optics, Fine Mechanics and Physics], [Ge Gao] at 03:22 13 April 2016

Gilbert, M., and Tyas, A. 2003. “Layout Optimization of Large-Scale Pin-Jointed Frames.” *Engineering Computations* 20 (8): 1044–1064.
Hemp, W. 1973. *Optimum Structures*. Oxford: Oxford University Press.
Kirsch, U. 1989. “Optimal Topologies of Truss Structures.” *Computer Methods in Applied Mechanics and Engineering* 72: 15–28.
Kirsch, U. 1990. “On Singular Topologies in Optimum Structural Design.” *Structural and Multidisciplinary Optimization* 2 (3): 133–142.
Liu, S., and H. Qiao. 2011. “Topology Optimization of Continuum Structures with Different Tensile and Compressive Properties in Bridge Layout Design.” *Structural and Multidisciplinary Optimization* 43 (3): 369–380.
Luenberger, D. G., and Y. Ye. 2008. *Linear and Nonlinear Programming*. Berlin: Springer.
Michell, A. G. M. 1904. “The Limits of Economy of Material in Frame-Structures.” *Philosophical Magazine Series 6* 8 (47): 589–597.
Nagtegaal, J. C., and Prager, W. 1973. “Optimal Layout of a Truss for Alternative Loads.” *International Journal of Mechanical Sciences* 15: 583–592.
Nori, V. V., and M. S. Tharval. 2007. “Design of Pile Caps—Strut and Tie Model Method.” *Indian Concrete Journal* 81 (4): 13–19.
Parkes, W. 1975. “Joints in Optimum Frameworks.” *International Journal of Solids and Structures* 11: 1017–1022.
Pritchard, T. J., M. Gilbert, and A. Tyas. 2005. “Plastic Layout Optimization of Large Scale Frameworks Subject to Multiple Load Cases, Member Self-Weight and with Joint Length Penalties.” In *6th World Congress of Structural Multidisciplinary Optimization*, May 30–June 3, Rio de Janeiro, Brazil.
Rozvany, G. I. N. 1996. “Some Shortcomings in Michell’s Truss Theory.” *Structural and Multidisciplinary Optimization* 12 (4): 244–250.
Rozvany, G. I. N. 1997. “Aims, Scope, Basic Concepts and Methods of Topology Optimization.” In *Topology Optimization in Structural Mechanics*, edited by G. I. N. Rozvany, 1–55. New York: Springer.
Rozvany, G. I. N. 2001. “On Design-Dependent Constraints and Singular Topologies.” *Structural and Multidisciplinary Optimization* 21 (2): 164–172.
Rozvany, G. I. N. 2011. *Structural Design via Optimality Criteria*. Dordrecht: Springer.
Rozvany, G. I. N., T. Sokół, and V. Pomezanski. 2014. “Fundamentals of Exact Multi-load Topology Optimization-Stress-Based Least-Volume Trusses (Generalized Michell Structures)—Part I: Plastic Design.” *Structural and Multidisciplinary Optimization* 50 (6): 1051–1078.
Smith, O. D. S. 1996. “An Interactive System for Truss Topology Design.” *Advances in Engineering Software* 27: 167–178.
Smith, O. D. S. 1998. “Generation of Ground Structures for 2D and 3D Design Domains.” *Engineering Computations* 15 (4): 462–500. (39).
Sokół, T. 2011a. “A 99 Line Code for Discretized Michell Truss Optimization Written in Mathematica.” *Structural and Multidisciplinary Optimization* 43 (2): 181–190.
Sokół, T. 2011b. “Topology Optimization of Large-Scale Trusses Using Ground Structure Approach with Selective Subsets of Active Bars.” In *19th International Conference on Computer Methods in Mechanics (CMM2011)*, May 9–12, Warsaw, Poland.
Sokół, T. 2014. “Multi-load Truss Topology Optimization Using the Adaptive Ground Structure Approach.” In *Recent Advances in Computational*, edited by T. Łodygowski, J. Rakowski, and P. Litewka, 9–16. London: CRC Press.
Sokół, T., and G. I. N. Rozvany. 2013. “Exact Least-Volume Trusses for Two Symmetric Point Loads and Unequal Permissible Stresses in Tension and Compression.” *Structural and Multidisciplinary Optimization* 47 (1): 151–155.
Sved, S., and Z. Ginos. 1968. “Structural Optimization Under Multiple Loading.” *International Journal of Mechanical Sciences* 10 (10): 803–805.
Tuchscherer, R. G., D. B. Birrcher, and O. Bayrak. 2011. “Strut-and-Tie Model Design Provisions.” *Pci Journal* 56 (1): 155–170.
Wei, P., H. Ma, and M. Y. Wang. 2014. “The Stiffness Spreading Method for Layout Optimization of Truss Structures.” *Structural and Multidisciplinary Optimization* 49 (4): 667–682.
Xu, X., and M. Yuan. 2005. “Automatic Portraying of Principal Stress Trace.” *Journal of Experimental Mechanics* 20 (1): 156–159.
Zegard, T., and G. H. Paulino. 2014. “GRAND—Ground Structure Based Topology Optimization for Arbitrary 2D Domains Using MATLAB.” *Structural and Multidisciplinary Optimization* 50 (5): 861–882.
Zhou, K. 2011. “Topology Optimization of Truss-Like Continua with Three Families of Members Model Under Stress Constraints.” *Structural and Multidisciplinary Optimization* 43 (4): 487–493.

Downloaded by [Changchun Institute of Optics, Fine Mechanics and Physics], [Ge Gao] at 03:22 13 April 2016